World Electric Vehicle Journal

MDPI

Article

Analytical Calculation of Mutual Inductance of Search Coils in Interior Permanent Magnet Synchronous Motor

Xinmin Li [1,2,*], Chenfeng Sun [1], Zhezhun Xu [3] and Chen Li [2]

[1] School of Electrical Engineering, Tiangong University, Tianjin 300387, China; 2131070896@tiangong.edu.cn
[2] Advanced Electrical Equipment Innovation Center, Zhejiang University, Hangzhou 311107, China; lichen_hz@zju.edu.cn
[3] Technical Center of Hangzhou Customs, Hangzhou 311200, China; xzz@zaiq.org.cn
* Correspondence: lixinmin@tju.edu.cn

Abstract: Inductance is an important parameter for motor design and control, and the performance of the motor is closely related to the inductance parameter. To solve the problem of the complex magnetic circuit structure of search coil mutual inductance, this paper takes an 8-pole and 48-slot interior permanent magnet synchronous motor (IPMSM) as the object to carry out the relevant research on the formula of search coil mutual inductance, illustrates the method of calculating the mutual inductance of the search coil, and compares and verifies the proposed method through finite element analysis and the actual measurement results. By setting up a procedure for calculating the magnetic flux of the search coil, the magnetic flux of each sub-coil of the search coil is analyzed and calculated. The mutual inductance of the search coil is calculated by summing up the magnetic chains of different sub-coils between the phases of the search coil. Lastly, the finite element simulation of the permanent magnet synchronous motor (PMSM) with the placement of the search coil is carried out, the inductance of the search coil in the experimental prototype is measured practically, and the finite element simulation results of the mutual inductance of the search coil are compared with the actual measurement results, which proves the correctness of the theoretical analysis.

Keywords: permanent magnet synchronous motor (PMSM); search coil; mutual inductance; finite element simulation

check for updates

Citation: Li, X.; Sun, C.; Xu, Z.; Li, C. Analytical Calculation of Mutual Inductance of Search Coils in Interior Permanent Magnet Synchronous Motor. *World Electr. Veh. J.* **2024**, *15*, 577. https://doi.org/10.3390/wevj15120577

Academic Editors: Emil Tudor, Lucian Pîslaru-Dănescu, Mihaita-Gabriel Neacsu and Zhongze Wu

Received: 12 November 2024
Revised: 3 December 2024
Accepted: 9 December 2024
Published: 14 December 2024

Copyright: © 2024 by the authors. Published by MDPI on behalf of the World Electric Vehicle Association. Licensee MDPI, Basel, Switzerland. This article is an open access article distributed under the terms and conditions of the Creative Commons Attribution (CC BY) license (https://creativecommons.org/licenses/by/4.0/).

1. Introduction

The interior permanent magnet synchronous motor (IPMSM) is widely used in the field of new energy vehicles, and the accurate acquisition of information on the electromechanical parameters of the permanent magnet synchronous motor (PMSM) is crucial for the design of high-performance controllers [1–3]. Most drive systems require accurate inductance measurements such as controller design, observer design, and rotor position estimation [4–6]. The change in the value of the d-q axis reluctance causes the inductance of the IPMSM to vary with the rotor position. Therefore, in order to obtain a better control system, it is necessary to investigate each specific value of the inductance parameter [7–9].

Typically, the PMSM is used mainly for position detection using position sensors such as optical electricity encoders, resolvers, and others [10,11]. However, the majority of position sensors are susceptible to harsh environments and difficult to install. Search coils have received a lot of attention due to their low cost and independence from temperature and harsh environments. The search coil is placed as an additional winding in the stator slot of the motor and can be used as a new type of position sensor [12,13]. The search coil is not only used to feedback rotor position information, but also for temperature detection [14], as well as for detecting the eccentricity of the motor rotor [15–18].

The inductance of the search coil is an important parameter for building accurate mathematical models and analyzing the performance of motors due to the fact that the search coil is mounted in the stator slot of the motor and its performance is utilized in the

process of motor-related design and control. The influence of the magnetic circuit saturation and the change in the magnetic circuit structure will result in the nonlinear variation of the inductance of the search coil, in which the mutual inductance of the search coil is more obviously affected by the saturation of the magnetic circuit and other factors. In the existing literature, the search coil can be used for rotor position estimation, which is combined with temperature detection by means of thermistors, and the inductance parameter of the search coil is utilized in the formula for deriving the position estimation result [19]. However, no specific expression has been established for the inductance parameter of the search coil, which would have an impact on the results of the position detection. Based on the literature [19], the position detection technique of the search coil is applied to the synchronous reluctance motor drive system; however, the expression for the inductance of the search coil is still not established [20]. Based on the mutual inductance effect between the search coil and the armature windings, rotor position detection can be performed while the motor is stationary [21]. However, this approach does not specifically analyze the inductance equation of the search coil. Based on the inductance variation of the search coil, the ultra-high-frequency (UHF) sinusoidal signal injection method has been used in the existing literature for PMSM position detection [22]. However, no specific formula for the mutual inductance of the search coil has been derived.

Therefore, the mutual inductance expression for the search coil is derived in this paper by analyzing an 8-pole, 48-slot PMSM with the search coil placed on it. To establish the sub-coil magnetic chain expression of the search coil, the mutual inductance magnetic chain formula of each sub-coil between different phases is calculated and analyzed, and then the sum of mutual inductance magnetic chain of the sub-coils between two phases of the search coil can be obtained as an expression of the mutual inductance of the search coil between the phases. Finally, by comparing the results of the finite element simulation of the mutual inductance of the search coil with the results of the actual measured mutual inductance parameters, the correctness of the theoretical and computational analyses is verified.

2. Design of Search Coil Mutual Inductance

2.1. Design Methods for Search Coils

The placement of the search coil in the motor is shown schematically in Figure 1. In Figure 1, the red L_A represents phase A of the armature winding; The green L_B represents phase B of the armature winding; The blue L_C represents phase C of the armature winding; And red L_a represents the search coil phase a; The green L_b represents the search coil phase b; The blue L_c represents the search coil phase c; The gray M_{ab}, M_{bc}, and M_{ca} represent the mutual inductance between search coils a and b, b and c, and c and a, respectively. The search coil is placed in the stator slot of the motor as an extra additional winding. In order to ensure the consistent rule of variation of the inductance of the search coil and that of the armature winding, it is necessary to align the three-phase axes of a, b, and c of the search coil with the three-phase axes of A, B, and C of the armature winding, respectively, in the process of the design of the search coil. The neutral point of the search coil exists independently from that of the armature winding.

A simplified schematic of the structure of the motor with the search coil installed is shown in Figure 2. As shown in Figure 2, the red A_1, A_2, A_3, and A_4 represent the 4 sub-coils composing phase A of the armature winding, the green B_1, B_2, B_3, and B_4 represent the 4 sub-coils composing phase B of the armature winding, and the blue C_1, C_2, C_3, and C_4 represent the 4 sub-coils composing the phase C of the armature winding. The red a_1, a_2, a_3, a_4 denote the 4 sub-coils of phase a of the search coil; the green b_1, b_2, b_3, b_4 denote the 4 sub-coils of phase b of the search coil; the blue c_1, c_2, c_3, c_4 denote the 4 sub-coils of phase c of the search coil. The three phases a, b, and c of the search coil are mounted on the outside of the stator slot, and the three phases A, B, and C of the armature winding are mounted on the inside of the stator slot. This installation can be reached by the search coil of the three-phase axis and armature winding three-phase axis in the same position,

and then can consistently realize the search coil inductance variation rule and armature winding inductance variation rule.

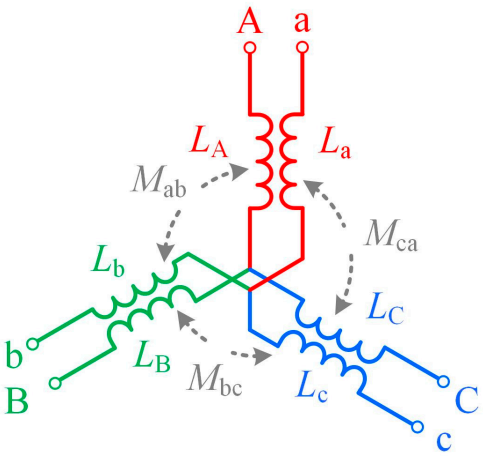


Figure 1. Schematic of search coil placement.

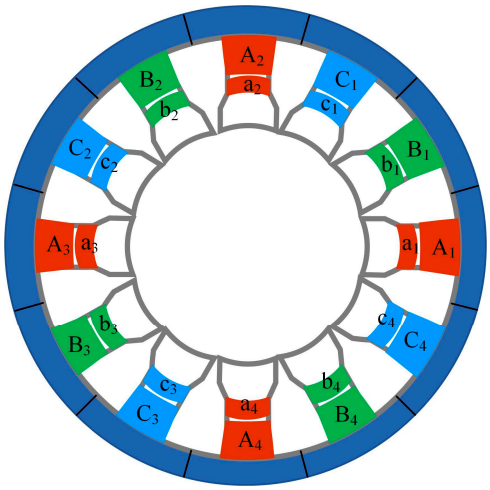


Figure 2. Schematic simplification of the motor structure including the search coil.

The search coil is placed in the stator slot of the motor, which takes up a certain amount of slot space, so it is necessary to calculate the slot fill factor after adding the search coil. Inductance is affected by the number of turns, wire diameter, and roots of the parallel winding of the search coil itself. The formula for the slot fill factor with the addition of the search coil is

$$sf_1 = \frac{N_s N_b (D_d + h_d)^2 + N_{s1} N_{b1} (D_{d1} + h_{d1})^2}{A_{ef}} \quad (1)$$

where sf_1 is the slot fill factor after placing the search coil; N_s is the number of conductors per slot of the armature winding; N_b is the number of parallel windings of the armature winding; D_d is the diameter of the enameled wire bare wire of the armature winding; h_d is the bilateral thickness of the insulating film corresponding to the enameled wire of the armature winding; A_{ef} is the effective slot area of the placed winding; N_{s1} is the number of conductors per slot of the search coil; N_{b1} is the root of the parallel winding of the search coil; D_{d1} is the bare wire diameter of the varnished wire of the search coil; and h_{d1} is the bilateral thickness of the insulating film corresponding to the varnished wire of the search coil. The parameters of the search coil are shown in Table 1.

Table 1. Parameters of search coil.

Parameters	Symbol	Value	Unit
Number of turns	N_{s1}	8	--
Number of parallel winding roots	N_{b1}	1	--
Bare wire diameter	D_{d1}	0.6	mm
Bilateral insulation thickness	h_{d1}	0.06	mm
Slot fill factor with search coil	sf_1	73%	--

2.2. Mutual Inductance Change Rule of the Search Coil

The IPMSM d-axis reluctance is greater than the q-axis reluctance, so the motor has the salient effect. The inductance of the nature of the magnetic circuit is determined by the physical structure of the magnetic circuit, and the size of the search coil inductance is then related to the position of the rotor. The corresponding relationship between search coil inductance and rotor position is shown in Figure 3. As can be seen from Figure 3, the inductance of the search coil changes with the rotor position with an approximate sinusoidal regularity. Its frequency of change and the operation of the motor frequency have a two-fold relationship, so determination of the rotor position of the motor can be based on the size of the mutual inductance of the search coil.

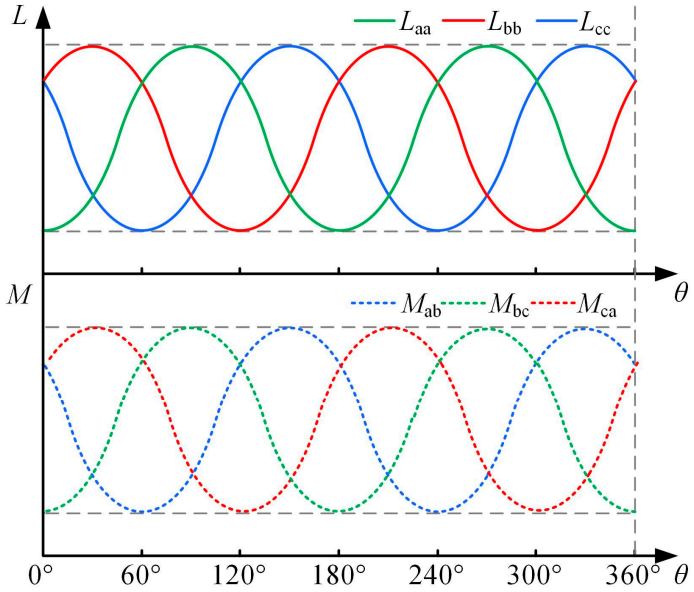


Figure 3. Diagram of search coil inductance about rotor position.

3. Optimization and Analytical Calculation of Search Coil Mutual Inductance

3.1. Optimized Design of Search Coil Mutual Inductance

The PMSM model containing the search coil was established in ANSYS Maxwell 2022 R1, and the cross-section of the finite element PMSM model is shown in Figure 4. In Figure 4, the black dashed box is labeled as the armature winding; the blue dashed box is labeled as the search coil. Phases A, B, and C represent the three phases of the armature winding, whose three phases are described as orange, emerald green, and red, respectively, using the colors in Figure 4; and phases a, b, and c represent the three phases of the search coil, whose three phases are described as purple, dark green, and pink, respectively, using the colors in Figure 4. Ink blue indicates the N pole of the permanent magnet; light blue indicates the S pole of the permanent magnet; light gray indicates the stator of the PMSM; dark gray indicates the rotor of the PMSM.

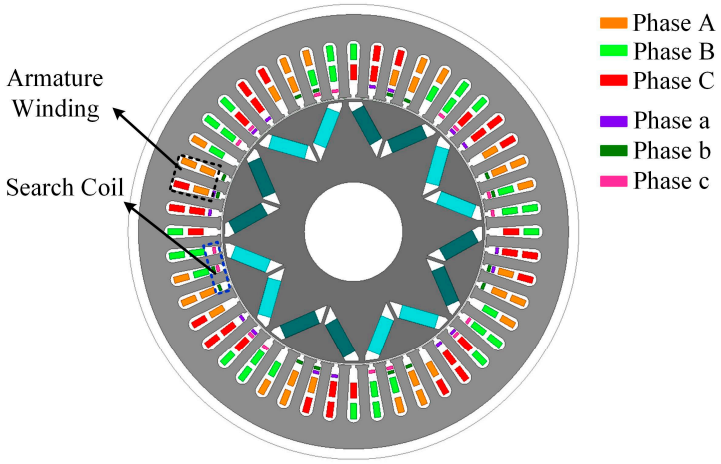


Figure 4. Structure and rotor cross-section of interior permanent magnet synchronous motors with search coils.

The structural parameters of the IPMSM designed in this paper are shown in Table 2.

Table 2. Structural parameters of IPMSM.

Parameters	Sizes
Rated speed	3000 r/min
Rated power	18 kW
Rated torque	58 N·m
D-axis inductance	0.158 mH
Q-axis inductance	0.292 mH
Poles pairs	4
slot number	48
Diameter of stator	130 mm
Diameter of rotor	128 mm
number of parallel branches	4
Number of conductors per slot	10
Number of parallel winding roots	7
Bare wire diameter	1 mm
Bilateral insulation thickness	0.06 mm
Permanent magnet thickness	6.5 mm
Permanent magnet width	39 mm
Length of permanent magnet	140 mm

The equivalent circuit connection between the phase a search coil and the phase A armature winding is shown in Figure 5. In Figure 5, "A-X" denotes phase A of the armature winding, and "a-x" denotes phase a of the search coil; "a_1~a_4" denotes the four sub-coils that are connected in series in counterclockwise order inside the motor to form phase a of the search coil. "*" indicates the homonymous ends. If the homonymous end of the sub-coil is on the same side as the homonymous end of the armature winding, the sub-coil is an "S" type sub-coil; otherwise, the sub-coil is an "N" type sub-coil.

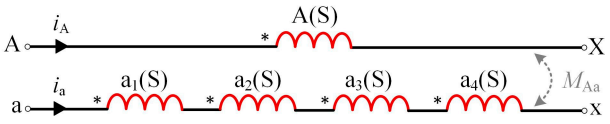


Figure 5. Equivalent circuit of phase a search coil and phase A armature winding.

The equivalent circuit of the three-phase search coil is shown in Figure 6.

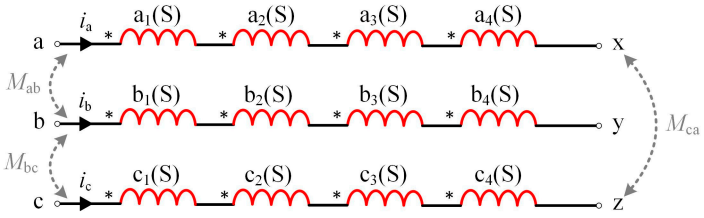


Figure 6. Equivalent circuit of three-phase search coil.

The individual sub-coils in the search coil have the same number of turns and pitch, and only their spatial position in the motor is different. The mutual inductance value between each sub-coil in the search coil will decrease with the increase in spatial distance. When analyzing the mutual inductance formula of the search coil, the mutual inductance value between this part of the sub-coils cannot be neglected, and the mutual inductance of the three-phase search coil can then be expressed as

$$\begin{cases} M_{\mathrm{ab}} = \sum\limits_{i=1}^{4}\sum\limits_{j=1}^{4} M_{\mathrm{a}_i\mathrm{b}_j} \\ M_{\mathrm{bc}} = \sum\limits_{i=1}^{4}\sum\limits_{j=1}^{4} M_{\mathrm{b}_i\mathrm{c}_j} \\ M_{\mathrm{ca}} = \sum\limits_{i=1}^{4}\sum\limits_{j=1}^{4} M_{\mathrm{c}_i\mathrm{a}_j} \end{cases} \tag{2}$$

From Equation (2), it can be seen that by connecting several sub-coils in series, the mutual inductance value of each phase of the search coil can be increased, which can satisfy the need for the mutual inductance value of the search coil of the PMSM.

3.2. Analytical Calculation of Mutual Inductance of Search Coils

The self-inductance of any coil is equal to the ratio of the increment of the self-inductive magnetic chain crossed by that coil to the increment of the current in the coil. When the permeability of the magnetic circuit through which it passes is linear, the self-inductance of the coil can be expressed as

$$L = \frac{\psi}{i} \tag{3}$$

where ψ is the self-inductance flux linkage of the coil and i is the current flowing through the coil.

The mutual inductance between two coils is expressed as a mutually induced magnetic chain generated by the current passed through one of the coils interlinked with another neighboring coil. Then the mutual inductance between any two coils can be expressed as

$$L_{\mathrm{k,j}} = \frac{\psi_{\mathrm{k,j}}}{i_{\mathrm{j}}} \tag{4}$$

where $\psi_{\mathrm{k,j}}$ is the magnetic chain generated by the j-coil current interlinked with the k-coil, and i_{j} is the j-coil current.

The salient effect of the PMSM results in a sinusoidal distribution of the inductance of the search coil. The starting position is the axis position of the phase a search coil, and the coil connection direction is counterclockwise in the positive direction. Then the number of conductor roots per unit radian of the phase a probe coil at the mechanical position x is

$$v_a(x) = v_0 \sin(px) \tag{5}$$

where v_0 is the root base value of the conductor per unit radian and p is the number of pole pairs of the motor.

The permeability of the permanent magnets of the IPMSMs can be approximated to be equal to the permeability of air. It is assumed that the PMSM is an ideal type of motor, which satisfies the following:

① The magnetic circuit inside the motor is linear, the eddy current loss and magnetic hysteresis in the iron core can be neglected, and the surface of the stator and rotor is smooth;

② The high harmonic of the air gap magnetic field is neglected, and the air gaps of the straight axis and cross-axis of the permanent magnet synchronous motors (PMSMs) are unequal, and the ratio of magnetic permeance of the air gap can be expressed by the average value adding the second harmonic.

Defining the magnetic circuit direction from the rotor pointing to the stator direction as the positive direction, as shown in Figure 7, with "×" indicating the current inflow direction and "·" indicating the current outflow direction, the magnetomotive force at the mechanical position x of the PMSM can be expressed as $F(x)$, and the magnetomotive force at the mechanical position $x + \Delta x$ is denoted as $F(x + \Delta x)$. When current i_a is passed to the phase a search coil, from the Amberg circulation theorem, the increment of the magnetomotive force per unit radian of the phase a search coil can be expressed as

$$F(x) - F(x + \Delta x) = i_a v_0 \sin(px)\Delta x \tag{6}$$

By transforming Equation (6), it is obtained that

$$\frac{F(x + \Delta x) - F(x)}{\Delta x} = -i_a v_0 \sin(px) \tag{7}$$

Then Equation (7) can be expressed as

$$F'(x) = -i_a v_0 \sin(px) \tag{8}$$

According to the equation of magnetomotive force, the magnetomotive force generated by the phase a search coil at $x = \pi/2p$ is 0.

$$F(\frac{\pi}{2p}) = 0 \tag{9}$$

Combining Equations (8) and (9), the expression for the magnetomotive force at the mechanical position x can be calculated as

$$F(x) = \frac{i_a v_0 \cos(px)}{p} \tag{10}$$

The magnetomotive force can be expressed as the ratio of the magnetic flux per unit area to the air gap permeability per unit area, where the magnetic flux per unit area is equal to the magnetic induction intensity. Therefore, the magnetic potential per unit area can be expressed as

$$F(x) = \frac{\phi(x)}{\Lambda(x)} = \frac{B(x)}{\Lambda(x)} \tag{11}$$

where $\phi(x)$ is the magnetic flux per unit area; $\Lambda(x)$ is the air gap magnetic permeance per unit area; and $B(x)$ denotes the magnetic induction per unit area.

According to Equation (11), the magnetic flux per unit area can be expressed as

$$B(x) = F(x)\Lambda(x) \tag{12}$$

As for the IPMSM, the air gap is always changing along the circumference of the rotor, so the air gap specific permeance is related to the rotor position of the motor. Since an ideal assumption is made for PMSMs, the air gap specific permeance can be expressed as

$$\Lambda(x) = \Lambda_0 - \Lambda_2 \cos[2p(x - \alpha)] \tag{13}$$

where Λ_0 is the constant component of the air gap magnetic conductance; Λ_2 is the amplitude of the second harmonic component of the air gap magnetic conductance; and α is the mechanical angle of the rotor.

During an electrical cycle of a PMSM, the current input to the sub-coil that forms the phase a search coil is denoted as x at the mechanical position of the motor, and the current outflow is denoted as $x + \pi/p$. Then the magnetic flux of a one-turn coil of two conductors at this position is

$$\phi(x) = \int_{x}^{x+\frac{\pi}{p}} B(x')Rl\mathrm{d}x' \tag{14}$$

where R is the radius at the stator air gap and l is the height of the motor.

When the current i_a is passed to the phase a probe coil, the magnetic chain of its phase a can be expressed as

$$\psi_{\mathrm{aa}} = p\int_{-\frac{\pi}{p}}^{0} \phi(x)(-v_0\sin(px))\mathrm{d}x \tag{15}$$

Combining Equations (3), (10), (12)–(15), an expression for the self-inductance of the phase a search coil is obtained as

$$L_{\mathrm{aa}} = \frac{v_0^2\pi Rl(2\Lambda_0 - \Lambda_2\cos(2p\alpha))}{2p^2} \tag{16}$$

The mutual inductance between any two phases of the search coil can be expressed as an accumulation of mutual inductance values between sub-coils of different phases. Then, according to Equation (4), the mutual inductance magnetic chain between the search coils can be expressed as

$$\begin{cases} \psi_{\mathrm{ab}} = \sum\limits_{i=1}^{4}\sum\limits_{j=1}^{4}\psi_{\mathrm{a}_i\mathrm{b}_j} \\ \psi_{\mathrm{bc}} = \sum\limits_{i=1}^{4}\sum\limits_{j=1}^{4}\psi_{\mathrm{b}_i\mathrm{c}_j} \\ \psi_{\mathrm{ca}} = \sum\limits_{i=1}^{4}\sum\limits_{j=1}^{4}\psi_{\mathrm{c}_i\mathrm{a}_j} \end{cases} \tag{17}$$

This paper analyzes and calculates the mutual inductance between phase a and phase b of the search coil as an example. The position of the phase b search coil axis is rotated counterclockwise by an electrical angle of $2\pi/3$ from the phase a search coil axis, which translates into the mechanical angle of $2\pi/3p$. Then the number of conductor roots per unit radian of the phase b search coil is

$$v_\mathrm{b}(x) = v_0\sin[p(x - \frac{2\pi}{3p})] \tag{18}$$

The magnetic flux relationship between the a1 sub-coil in phase a of the search coil and each sub-coil in phase b of the search coil is

$$\sum_{i=1}^{4}\psi_{\mathrm{a}_1\mathrm{b}_i} = \psi_{\mathrm{a}_1\mathrm{b}_1} + \psi_{\mathrm{a}_1\mathrm{b}_2} + \psi_{\mathrm{a}_1\mathrm{b}_3} + \psi_{\mathrm{a}_1\mathrm{b}_4} \tag{19}$$

For the a_1 sub-coil placed in the permanent magnet synchronous motor model designed in this article, the magnetic flux of the a_1 sub-coil can be calculated by combining Equations (12)–(14) as

$$\phi_{\mathrm{a}1}(x) = \int_{x}^{x+\frac{5\pi}{48}} \frac{i_\mathrm{a}v_0\cos(4x')}{4}(\Lambda_0 - \Lambda_2\cos(8(x'-\alpha)))Rl\mathrm{d}x' \tag{20}$$

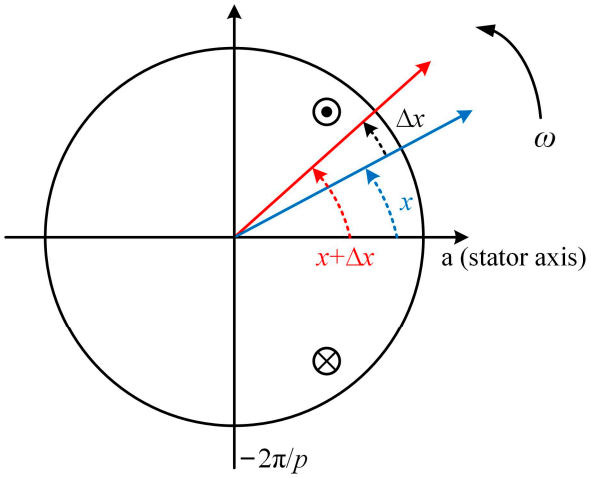


Figure 7. Schematic diagram of simplified mathematical model of PMSM.

As for the b_1, b_2, b_3, and b_4 sub-coils placed to form the phase b search coil in the PMSM model, the mutual inductance magnetic chain between each of them with the a_1 sub-coils can be obtained by combining Equations (18)–(20) to obtain

$$\begin{aligned}\sum_{i=1}^{4}\psi_{a_1b_i} &= \psi_{a_1b_1}+\psi_{a_1b_2}+\psi_{a_1b_3}+\psi_{a_1b_4}\\ &= \int_{\frac{\pi}{16}}^{\frac{\pi}{6}}\phi_{a1}(-v_0\sin(4(x-\frac{\pi}{6})))dx+\int_{\frac{9\pi}{16}}^{\frac{2\pi}{3}}\phi_{a1}(-v_0\sin(4(x-\frac{\pi}{6})))dx\\ &+\int_{\frac{17\pi}{16}}^{\frac{7\pi}{6}}\phi_{a1}(-v_0\sin(4(x-\frac{\pi}{6})))dx+\int_{\frac{25\pi}{16}}^{\frac{5\pi}{3}}\phi_{a1}(-v_0\sin(4(x-\frac{\pi}{6})))dx\end{aligned} \tag{21}$$

Similarly, according to the different positions of the a_2, a_3, and a_4 sub-coils in the motor, and combined with Equation (20), the magnetic flux of the a_2, a_3, and a_4 sub-coils can be calculated separately, as well as the mutual inductance magnetic flux between them and the search coil phase b sub coils.

Finally, the mutual inductance between phases a and b of the search coil can be summed as

$$\begin{aligned}M_{ab} &= \tfrac{(-6(2+\sqrt{2})(1+\sqrt{3})+5(-2+\sqrt{2}+\sqrt{6})\pi)Rl\Lambda_0v_0^2}{384}\\ &+\tfrac{Rlv_0^2}{384}\Lambda_2(-10\pi\cos(\tfrac{\pi}{12}-8\alpha)+12\cos(\tfrac{\pi}{6}-8\alpha)+(4+5\pi)\cos(8\alpha)\\ &+(-4-2\sqrt{3})\cos(\tfrac{\pi}{12}+8\alpha)-2\cos(\tfrac{\pi}{6}+8\alpha)+12\cos(\tfrac{\pi}{4}+8\alpha)+\\ &12\sin(\tfrac{\pi}{12}-8\alpha)+(2+8\sqrt{3}-5\sqrt{3}\pi)\sin(8\alpha))\end{aligned} \tag{22}$$

Since the number of pole pairs of the PMSM model designed in this paper is 4, it can be substituted into Equation (16) to obtain the search coil phase a self-inductance as

$$L_{aa} = \frac{\pi}{16}v_0^2Rl\Lambda_0 - \frac{v_0^2Rl}{32}\Lambda_2\cos(2\theta) \tag{23}$$

Let $\frac{\pi}{16}v_0^2Rl\Lambda_0$ in Equation (23) be L_{aa0}, and let $\frac{v_0^2Rl}{32}\Lambda_2$ in Equation (23) be L_{g2}.

Then by simplifying and calculating the equivalence of the expressions of mutual inductance between phases a and b of the search coil in Equation (22), the relation between mutual inductance between phases a and b and self-inductance of phase a can be approximated as

$$M_{ab} = -0.4L_{aa0} - 0.9L_{g2}\cos(2\theta - 2\pi/3) \tag{24}$$

Similarly, by repeating the above procedure of calculating the self-inductance of phase a of the search coil and the mutual inductance formula between phases a and b, the expressions for the self-inductance of phases b and c of the search coil and the mutual inductance between phases b and c and between phases c and a can be calculated separately. Then the expression for the inductance of the search coil can be obtained as

$$\begin{cases} L_{aa}(\theta) = L_{aa0} + L_{a1} - L_{g2}\cos(2\theta) \\ L_{bb}(\theta) = L_{aa0} + L_{a1} - L_{g2}\cos(2\theta + 2\pi/3) \\ L_{cc}(\theta) = L_{aa0} + L_{a1} - L_{g2}\cos(2\theta - 2\pi/3) \\ M_{ab}(\theta) = M_{ba}(\theta) = -0.4L_{aa0} - 0.9L_{g2}\cos(2\theta - 2\pi/3) \\ M_{bc}(\theta) = M_{cb}(\theta) = -0.4L_{aa0} - 0.9L_{g2}\cos(2\theta) \\ M_{ca}(\theta) = M_{ac}(\theta) = -0.4L_{aa0} - 0.9L_{g2}\cos(2\theta + 2\pi/3) \end{cases} \quad (25)$$

In Equation (25), L_{aa}, L_{bb}, and L_{cc} are the self-inductances of the search coils of phases a, b, and c, respectively; M_{ab}, M_{bc}, and M_{ca} are the mutual inductances between the three phases of the search coils, respectively; L_{aa0} is the inductive component due to the motor air gap magnetic field; L_{a1} is the inductance component due to the leakage flux of the motor; L_{g2} is the amplitude of the second harmonic component of the self-inductance of the search coil; and θ is the electrical angle of the rotor.

4. Finite Element Simulation and Experimental Results Analysis

4.1. Finite Element Simulation Analysis

An 8-pole 48-slot PMSM model containing search coils was established in ANSYS Maxwell. The motor parameters are shown in Table 2, and the magnetic density distribution of the PMSM model can be obtained as shown in Figure 8.

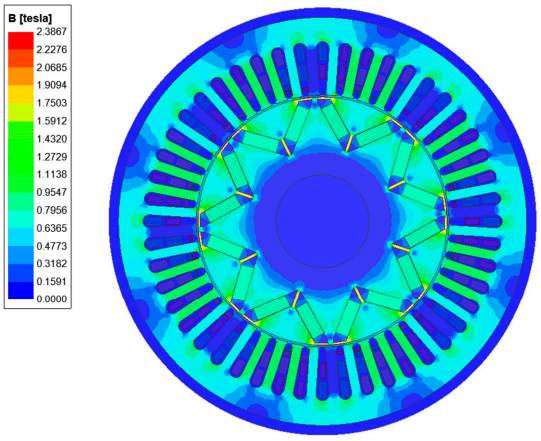


Figure 8. The magnetic density of cloud atlas.

The definition of the boundary is a very critical step when constructing a 2D PMSM model in ANSYS Maxwell. The setting of boundary conditions usually involves the geometry of the stator and rotor in order to carry out calculations of the current distribution and magnetic field. In this paper, we choose the vector potential boundary condition, which defines the constant value of the vector potential on the boundary, so as to ensure that the magnetic field at the boundary is tangent to the boundary. Then it can be ensured that the magnetic field is strictly confined within the boundary and will not leak out of the boundary. Since the PMSM model established in this paper adopts a full-domain computational model, it only needs to set boundary conditions on the outer circle of the stator. The permeability of ferromagnetic materials such as the iron core in the motor model is much larger than the air permeability, and it can be assumed that there is very little magnetic leakage in the motor, so the outer circle of the motor stator can be used as the boundary of the solution domain. This article uses Maxwell's adaptive partitioning function to partition the solution area. In this paper, the transient solution was selected in

Maxwell's solution type, the solution step size was set to 0.1 ms, and the time was set to 5 ms. With this solution, the transient response of some parameters of the motor, such as current and flux, can be displayed for a given condition.

Through finite element simulation of the PMSM model, the schematic waveforms of search coil self-inductance and mutual inductance in one electrical cycle can be obtained, as shown in Figure 9.

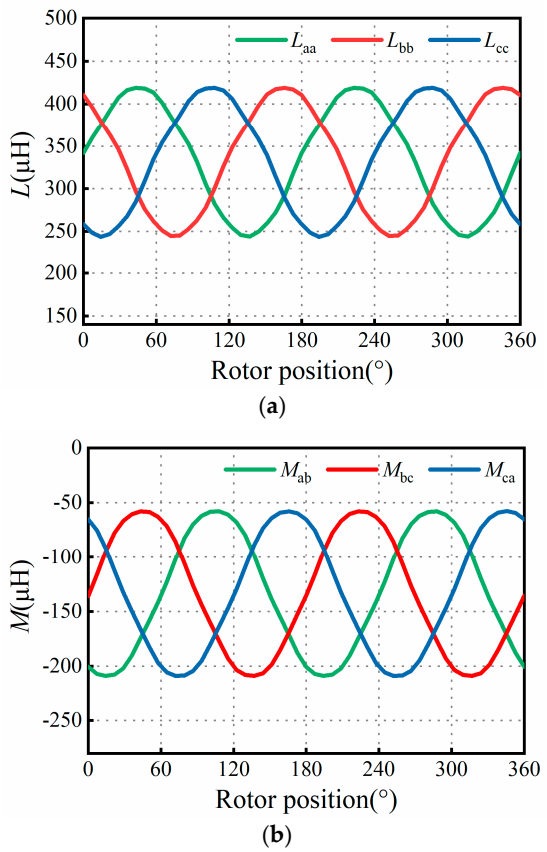


Figure 9. The waveforms of finite element simulation of self-inductance and mutual inductance of search coil. (**a**) The waveform of finite element simulation of search coil self-inductance; (**b**) the waveform of finite element simulation of search coil mutual inductance.

As shown in Figure 9a, the finite element simulation waveform of the search coil's self-inductance shows that the search coil's three-phase self-inductance waveform exhibits sinusoidal regularity within one electrical cycle. The amplitude L_{g2} of the second harmonic component of self-inductance is 87.51 μH and the inductance component L_{aa0} caused by the air gap magnetic field is 331.24 μH. As shown in Figure 9b, the waveforms of the mutual inductance of the search coil are sinusoidally and symmetrically distributed in one electrical cycle and show sinusoidal regularity with the rotor position. From the finite element simulation waveforms of the mutual inductance of the search coil, it can be concluded that the second harmonic component amplitude M_{g2} of the three mutual inductances is 75.49 μH, while the mutual inductance component M_{aa0} caused by the air gap magnetic field is 133.3 μH.

By analyzing and calculating the finite element simulation results of the self-inductance and mutual inductance waveforms of the search coil, it can be concluded that the mutual inductance component M_{aa0} caused by the air gap magnetic field of the mutual inductance of the search coil is about 0.41 times the self-inductance L_{aa0}, and the amplitude M_{g2} of the second harmonic component of mutual inductance is about 0.86 times that of the amplitude L_{g2} of the second harmonic component of self-inductance. From the results obtained in this paper for the analytical calculation of the mutual inductance of the search coil, the mutual

inductance component M_{aa0} due to the air gap magnetic field of the mutual inductance of the search coil is about 0.4 times the self-inductance L_{aa0}, and the amplitude of the second harmonic component M_{g2} of mutual inductance is about 0.9 times the amplitude of the second harmonic component L_{g2} of self-inductance. The differences between the analytical calculation results and the finite element simulation are small and in accordance with the theoretical values, which verifies the correctness of the derived formula for the mutual inductance of the search coil.

Finite element simulation is used to analyze the effect of magnetic hysteresis loss and eddy current loss on the proposed method, and the results of the finite element analysis are given in Figure 10. Figure 10a shows the simulation results of search coil self-inductance and mutual inductance when the core magnetic hysteresis loss and eddy current loss are not set, and Figure 10b shows the simulation results of search coil self-inductance and mutual inductance when the core magnetic hysteresis loss and eddy current loss are set. From the comparison of Figure 10a,b, it can be seen that the values of self-inductance and mutual inductance of the search coils are not affected by the magnetic hysteresis loss, and the eddy current loss of the iron core is limited and negligible. Therefore, in order to simplify the mathematical model of the search coil, the eddy current loss and magnetic hysteresis of the iron core are neglected in this paper when deriving the equation.

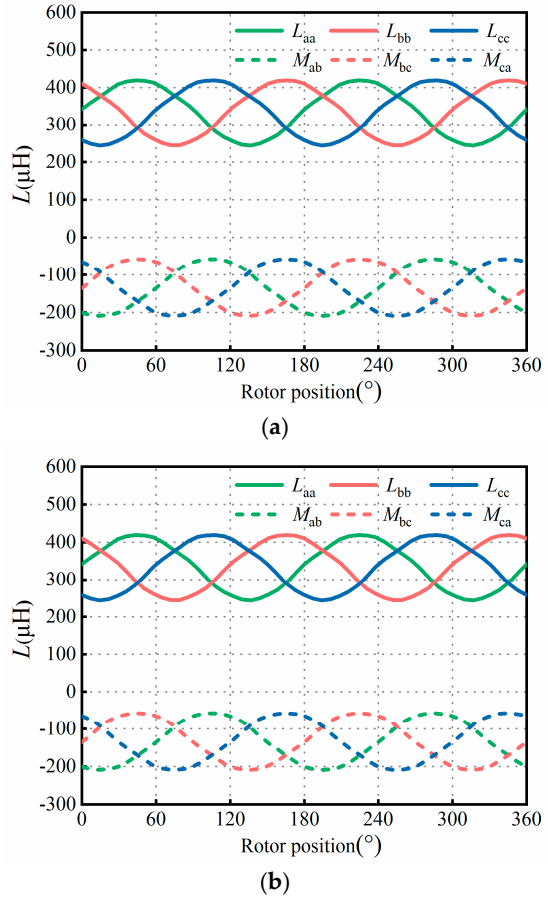


Figure 10. The figure of finite element simulation results of self-inductance and mutual inductance of the search coil. (**a**) Finite element simulation results of search coil inductance without setting magnetic hysteresis loss and eddy current loss of iron core; (**b**) finite element simulation results of search coil inductance with setting magnetic hysteresis loss and eddy current loss in the iron core.

4.2. Analysis of Experimental Measurement Results

A PMSM containing a search coil is fabricated in this paper, and its appearance is shown in Figure 11 with a partial schematic of the stator. For the experimental prototype, the armature winding is an integer-slot double-layer distributed winding with pitch = 5,

number of parallel branches = 4, number of turns = 10, and wire diameter = 1.06 mm. The winding of the search coil is the same as the armature winding, the number of turns of the search coil is 8, and the wire diameter is 0.66 mm. The parameters of the experimental prototype are shown in Table 2.



Figure 11. The physical picture of the experimental prototype.

In order to verify the correctness of the theoretical analysis and the effectiveness of the proposed analytical calculation method for the mutual inductance of the search coil, the inductance of the search coil in the experimental prototype is measured. The core part of the PMSM system controller of this experiment is the DSP main program, which mainly includes the initialization program, the revolver decoding, etc. The inductance of the search coil of the experimental prototype was measured by an LCR meter (E4980AL) manufactured by KEYSIGHT, and the measurement frequency of the LCR meter was set to 100 kHz because this paper mainly focuses on the search coil of the UHF sinusoidal signal injection method for the detection of the rotor position of the motor. The rotor position of the experimental prototype was measured by the resolver.

The motor position was fixed at the initial position of 0 degrees for one of the electrical cycles by manually rotating the shaft extension end position of the PMSM. The self-inductance value of phase a of the search coil is recorded every three degrees of electrical rotation until the end of an electrical cycle. Similarly, in the same electrical cycle, the same method is used to record the self-inductance values of phase b and phase c search coils, from which the self-inductance values of the search coils a, b, and c can be obtained. Since the mutual inductance value of the search coil cannot be measured directly, the line inductance of phases ab, bc, and ca of the search coil can be recorded in the same electrical cycle in the manner described above, and the three mutual inductance measurements of the search coil can be obtained by calculating according to Equation (26).

$$\begin{cases} M_{ab} = (L_a + L_b - L_{ab})/2 \\ M_{bc} = (L_b + L_c - L_{bc})/2 \\ M_{ca} = (L_c + L_a - L_{ca})/2 \end{cases} \tag{26}$$

where L_{ab}, L_{bc}, and L_{ca} are the line inductance values of the ab, bc, and ca phases of the search coil, respectively.

By measuring the value of self-inductance and mutual inductance of the search coil of the experimental prototype, the waveform graph can be obtained as shown in Figure 12. Figure 12a shows the actual measured waveform of the self-inductance of the search coil, with the self-inductance of the search coil exhibiting sinusoidal regularity with the rotor position in one electrical cycle. From the measurements, it is obtained that the inductance component L_{aa0} due to the air gap magnetic field is 276.75 μH, while the amplitude of the second harmonic component L_{g2} of the self-inductance is 73.25 μH. According to the actual measurement waveform of the search coil mutual inductance in Figure 12b, it can be seen that the mutual inductance component M_{aa0} caused by the air gap magnetic field is 97.23 μH, while the amplitude of the second harmonic component M_{g2} of the three-phase mutual inductance is 61.58 μH.

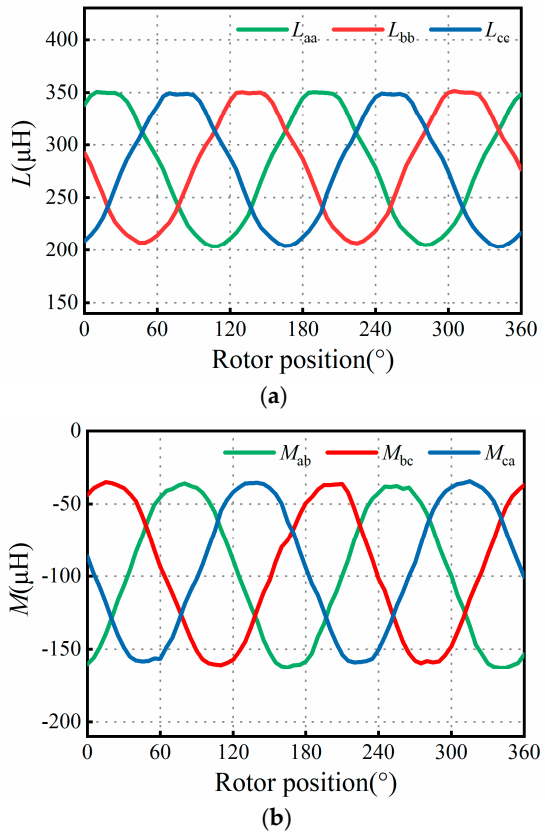


Figure 12. The actual measured waveforms of the self-inductance and mutual inductance of the search coil. (**a**) The actual measured waveform of the search coil self-inductance; (**b**) the actual measured waveform of the search coil mutual inductance.

From the actual measurement results of the self-inductance and mutual inductance waveforms of the search coil, it can be concluded that the inductance component M_{aa0} caused by the air gap magnetic field of the mutual inductance of the search coil is about 0.35 times the self-inductance L_{aa0}, and the amplitude M_{g2} of the second harmonic component of mutual inductance is about 0.84 times that of the amplitude L_{g2} of the second harmonic component of self-inductance. The measured inductance value is basically consistent with the inductance value analyzed by finite element simulation, and the error difference with the analytical calculation result of mutual inductance is relatively small, thus verifying the correctness of the theoretical analysis.

5. Conclusions

In this paper, an analytical calculation method for search coil mutual inductance of the IPMSM is proposed. In the process of motor-related control using search coils, the search coil inductance is an important parameter for building mathematical models and analyzing motor performance. In the existing literature related to rotor position detection using search coils, there has not been any research on the expression related to the inductance of the search coil. Based on this, this paper solves the problem of not having an accurate description of the expression of the mutual inductance magnetic circuit of the search coil due to its complexity. The accuracy of the analytical calculation method of this paper is verified by finite element analysis and experimental measurements, and the analytical calculation method of mutual inductance of the search coil proposed in this paper can be applied to the rotor position detection method using the inductance of the search coil, which is valuable in the field of motor control. The analytical calculation of mutual inductance in this paper is based on a linear magnetic circuit. However, the permanent magnet synchronous motor is a strongly coupled complex nonlinear system in actual operation. Therefore, to enhance

the accuracy of the mutual inductance calculation further, it is worthwhile to consider the influence of nonlinear factors such as magnetic field saturation on the mutual inductance calculation of the search coil for further research in the future.

Author Contributions: Data curation, X.L.; formal analysis, X.L. and C.S.; funding acquisition, X.L.; investigation, Z.X. and C.L.; methodology, C.S.; project administration, X.L. and C.L.; resources, Z.X.; validation, C.S.; writing—original draft, C.S.; writing—review and editing, X.L. All authors have read and agreed to the published version of the manuscript.

Funding: This research was supported by "Zhejiang Provincial "Pioneer" and "Leading Goose" R&D Program of China under grant numbers 2023C01134", "The National Natural Science Foundation of China, grant number 52477060".

Data Availability Statement: The original contributions presented in the study are included in the article, further inquiries can be directed to the corresponding author.

Conflicts of Interest: Zhezhun Xu is an employee of Technical Center of Hangzhou Customs. The paper reflects the views of the scientists and not the organization.

Nomenclature

A. List of Acronyms	
IPMSM	Interior Permanent Magnet Synchronous Motor
PMSM	Permanent Magnet Synchronous Motor
UHF	Ultra-High Frequency
IPMSMs	Interior Permanent Magnet Synchronous Motors
PMSMs	Permanent Magnet Synchronous Motors
B. List of Symbols	
N_s	Number of conductors per slot of armature winding
N_b	The number of parallel winding roots of armature winding
D_d	Diameter of enameled wire bare wire of armature winding
h_d	The thickness of the insulation film on both sides corresponding to the enameled wire of the armature winding
A_{ef}	Effective slot area for placing windings
sf_1	The slot fill factor after placing the search coil
N_{s1}	The number of conductors per slot of the search coil
N_{b1}	The root of the parallel winding of the search coil
D_{d1}	The bare wire diameter of the varnished wire of the search coil
h_{d1}	The bilateral thickness of the insulating film corresponding to the varnished wire of the search coil
M_{ab}, M_{bc}, M_{ca}	Three mutual inductance of search coil
ψ	The self-induced magnetic flux of the coil
i	Current flowing through the coil
$\psi_{k,j}$	The magnetic chain generated by the *j*-coil current interlinked with the *k*-coil
i_j	*j*-coil current
x	Mechanical position
v_0	The root base value of the conductor per unit radian
p	Motor pole pairs
$F(x)$	The magnetomotive force at the mechanical position x of the PMSM
i_a	Search coil phase a current
Δx	Mechanical position increment
$\phi(x)$	Magnetic flux per unit area
$\Lambda(x)$	Air gap permeance per unit area
$B(x)$	Magnetic induction intensity per unit area
Λ_0	Air gap permeance constant component
Λ_2	Amplitude of second harmonic component of air gap permeance
α	Rotor mechanical angle

ψ_{aa}	The flux linkage of the search coil phase a
R	Radius of stator air gap
l	Linear motor height
ψ_{ab}, ψ_{bc}, ψ_{ca}	The ab, bc, ca phase magnetic chains of the search coil
ψ_{a1b1}, ψ_{a1b2}, ψ_{a1b3}, ψ_{a1b4}	The flux linkage between the detection coil a_1 subcoils and the b_1~b_4 sub-coils respectively.
L_{aa}, L_{bb}, L_{cc}	Three-phase self-inductance of search coil
L_{ab}, L_{bc}, L_{ca}	Three-phase line inductance of search coil
L_{aa0}	Inductance component caused by air gap magnetic field of motor
L_{a1}	Inductance component caused by leakage flux of motor
L_{g2}	The amplitude of the second harmonic component of the self inductance of the search coil
θ	Electrical angle of the rotor

References

1. Luan, M.; Zhang, Y.; Li, X.; Xu, F. A Rotor Position Detection Method for Permanent Magnet Synchronous Motors Based on Variable Gain Discrete Sliding Mode Observer. *World Electr. Veh. J.* **2024**, *15*, 87. [CrossRef]
2. Lin, Y.-S.; Yang, C.-W.; Liaw, C.-M.; Chiang, C.-L.; Liu, Y.-G.; Wang, C.-C. Development and Control of PMSM Drive with Improved Performance Over Wide Speed and Load Ranges. *IEEE Access* **2024**, *12*, 97154–97170. [CrossRef]
3. Wang, G.-L.; Kuang, J.-Y.; Zhao, N.-N.; Zhang, G.-Q.; Xu, D.-G. Rotor Position Estimation of PMSM in Low-Speed Region and Standstill Using Zero-Voltage Vector Injection. *IEEE Trans. Power Electron.* **2018**, *33*, 7948–7958. [CrossRef]
4. Lee, C.-H.; Huang, H.-J.; Chang, J.-P.; Chen, Y.-C. Incremental Optical Encoder Based on a Sinusoidal Transmissive Pattern. *IEEE Photon. J.* **2022**, *14*, 1–6. [CrossRef]
5. Wang, Z.; Yao, B.; Guo, L.; Jin, X.; Li, X.; Wang, H. Initial Rotor Position Detection for Permanent Magnet Synchronous Motor Based on High-Frequency Voltage Injection without Filter. *World Electr. Veh. J.* **2020**, *11*, 71. [CrossRef]
6. Chen, B.; Chang, J.-Y. Effect of Flattening Cracked Medium on Positioning Accuracy of a Linear Magnetic Encoder. *IEEE Trans. Magn.* **2020**, *56*, 1–7. [CrossRef]
7. Li, C.; Kudra, B.; Balaraj, V.; Akin, B. Absolute Inductance Estimation of PMSM Considering High-Frequency Resistance. *IEEE Trans. Energy Convers.* **2021**, *36*, 91–94. [CrossRef]
8. Mukundan, S.; Dhulipati, H.; Iyer, K.L.V.; Kar, N.C.; Mukherjee, K. Comparison of inductance determination methods of PMSMs for EV application. Proceeding of the 2017 IEEE 30th Canadian Conference on Electrical and Computer Engineering (CCECE), Windsor, ON, Canada, 30 April–3 May 2017; pp. 1–4.
9. Boztas, G.; Aydogmus, O. Design of a High-Speed PMSM for Flywheel Systems. Proceeding of the 4th International Conference on Power Electronics and their Applications (ICPEA), Elazig, Turkey, 25–27 September 2019; pp. 1–5.
10. Sun, L.; Taylor, J.; Callegaro, A.-D.; Emadi, A. Stator-PM-Based Variable Reluctance Resolver With Advantage of Motional Back-EMF. *IEEE Trans. Ind. Electron.* **2020**, *67*, 9790–9801. [CrossRef]
11. Chang, T.-W.; Huang, P.-W.; Huang, W.-C.; Huang, C.-C.; Mo, C.-C.; Tsai, M.-C. Additive Manufacturing High Fault-Tolerant Axial Flux Variable Reluctance Resolver. *IEEE Trans. Magn.* **2023**, *59*, 1–5. [CrossRef]
12. Da, Y.; Shi, X.; Krishnamurthy, M. A New Approach to Fault Diagnostics for Permanent Magnet Synchronous Machines Using Electromagnetic Signature Analysis. *IEEE Trans. Power Electron.* **2013**, *28*, 4104–4112. [CrossRef]
13. Da, Y.; Shi, X.; Krishnamurthy, M. A Novel Universal Sensor Concept for Survivable PMSM Drives. *IEEE Trans. Power Electron.* **2013**, *28*, 5630–5638. [CrossRef]
14. Lee, H.-J.; Jeong, J.; Zapico, M.O.; Lee, S.B.; Reigosa, D.D.; Blanco, F.B.d. Airgap Flux Search Coil-Based Estimation of Permanent Magnet Temperature for Thermal Protection of PMSMs. *IEEE Trans. Ind. Appl.* **2024**, *60*, 367–376. [CrossRef]
15. Im, J.-H.; Kang, J.-K.; Hur, J. Static and Dynamic Eccentricity Faults Diagnosis in PM Synchronous Motor Using Planar Search Coil. *IEEE Trans. Ind. Electron.* **2023**, *70*, 9291–9300. [CrossRef]
16. Petrinić, M.; Tvorić, S.; Plavec, E.; Zrakić, B. Distinction of Asymmetric Load From Eccentricity or Synchronous Electric Generator Winding Fault Using Search Coil Measurements. *IEEE Trans. Ind. Appl.* **2021**, *57*, 4776–4785. [CrossRef]
17. Rafaq, M.-S.; Lee, H.-J.; Park, Y.; Lee, S.-B.; Zapico, M.-O.; Fernandez, D. Airgap Search Coil Based Identification of PM Synchronous Motor Defects. *IEEE Trans. Ind. Electron.* **2022**, *69*, 6551–6560. [CrossRef]
18. Skarmoutsos, G.-A.; Gyftakis, K.-N.; Rasid, S.-A.; Mueller, M. General Diagnostics in Direct-Drive Permanent-Magnet Synchronous Generators Using Two Magnetically-Coupled Search-Coils. *IEEE Trans. Ind. Appl.* **2024**, *60*, 278–288.
19. Scelba, G.; Tornello, L.-D.; Scarcella, G.; Cacciato, M.; Testa, A. Combined Rotor Position Estimation and Temperature Monitoring in Sensorless Synchronous Motor Drives. Proceeding of the 2018 IEEE 9th International Symposium on Sensorless Control for Electrical Drives (SLED), Helsinki, Finland, 13–14 September 2018; pp. 30–35.
20. Tornello, L.-D.; Scelba, G.; Scarcella, G.; Cacciato, M.; Testa, A.; Foti, S. Combined Rotor-Position Estimation and Temperature Monitoring in Sensorless, Synchronous Reluctance Motor Drives. *IEEE Trans. Ind. Appl.* **2019**, *55*, 3851–3862. [CrossRef]

21. Kwon, Y.-C.; Sul, S.-K.; Baloch, N.A.; Morimoto, S.; Ohto, M. Design, Modeling, and Control of an IPMSM With an Asymmetric Rotor and Search Coils for Absolute Position Sensorless Drive. *IEEE Trans. Ind. Appl.* **2016**, *52*, 3839–3850. [CrossRef]
22. Li, X.; Wang, H.; Wang, H.; Guo, L.; Chen, W. Designing Ultrahigh Frequency Motor Rotor Position Search Coils for Electric Propulsion in Drones. *Drones* **2023**, *7*, 181. [CrossRef]

Disclaimer/Publisher's Note: The statements, opinions and data contained in all publications are solely those of the individual author(s) and contributor(s) and not of MDPI and/or the editor(s). MDPI and/or the editor(s) disclaim responsibility for any injury to people or property resulting from any ideas, methods, instructions or products referred to in the content.